2023

Direct Observation of the Magnetic Anisotropy of an Fe (II) Spin Crossover Molecular Thin Film

Ashley S. Dale

Saeed Yazdani

Thilini K. Ekanayaka

Esha Mishra

Yuchen Hu

See next page for additional authors

Authors

Ashley S. Dale, Saeed Yazdani, Thilini K. Ekanayaka, Esha Mishra, Yuchen Hu, Peter A. Dowben, John W. Freeland, Jian Zhang, and Ruihua Cheng

JPhys Materials

ACCEPTED MANUSCRIPT • OPEN ACCESS

Direct observation of the magnetic anisotropy of an Fe (II) spin crossover molecular thin film

To cite this article before publication: Ashley S. Dale *et al* 2023 *J. Phys. Mater.* in press https://doi.org/10.1088/2515-7639/ace21a

IOP Publishing Journal Title
Journal **XX** (XXXX) XXXXXX https://doi.org/XXXX/XXXX

Direct Observation of the Magnetic Anisotropy of an Fe (II) Spin Crossover Molecular Thin Film

Ashley S. Dale[1], Saeed Yazdani[1], Thilini K. Ekanayaka[2], Esha Mishra[2], Yuchen Hu[4], Peter A. Dowben[2], John W. Freeland[3], Jian Zhang[5], and Ruihua Cheng[1]

[1] Department of Physics, Indiana University Purdue University Indianapolis, Indianapolis, USA
[2] Department of Physics and Astronomy, University of Nebraska, Lincoln, USA
[3]X-ray Science Division, Argonne National Laboratory, Argonne, USA
[4]Department of Chemistry, University of Nebraska, Lincoln, USA
[5]Molecular Foundry, Lawrence Berkeley National Laboratory, USA

E-mail: rucheng@iupui.edu

Received xxxxxx
Accepted for publication xxxxxx
Published xxxxxx

Abstract

Spin crossover molecules are a promising candidate for molecular spintronics that aim for ultrafast and low-power devices for data storage and magnetic and information sensing. The rapid spin state transition is best controlled by non-thermal methods including magnetic field. Unfortunately, the magnetic field normally required to switch the spin state is normally high (~30 T), which calls for better understanding of the fundamental mechanism. In this work, we provide clear evidence of magnetic anisotropy in the local orbital moment of a molecular thin film based on spin crossover complex $[Fe(H_2B(pz)_2)_2(bipy)]$ (pz = pyrazol−1−yl, bipy = 2,2'−bipyridine). Field dependent X-ray magnetic circular dichroism measurements indicate that the magnetic easy axis for the orbital moment is along the surface normal direction. Along with the presence of a critical field, our observation points to the existence of an anisotropic energy barrier in the high-spin state. The estimated nonzero coupling constant of $\sim 2.47 \times 10^{-5}$ eV molecule^{-1} indicates that the observed magnetocrystalline anisotropy is mostly due to spin-orbit coupling. The spin- and orbital-component anisotropies are determined to be 30.9 and 5.04 meV molecule^{-1}, respectively. Furthermore, the estimated *g* factor in the range of 2.2-2.45 is consistent with the expected values. This work has paved the way for an understanding of the spin-switching mechanism in the presence of magnetic perturbations.

Keywords: anisotropy, g factor, magnetic properties, spin crossover, spin transitions

1. Introduction

Some of the transition metal complexes exhibit a spin state transition between a high-spin state and a low-spin state due to external stimuli. Spin crossover (SCO) materials, in particular the molecule $[Fe(H_2B(pz)_2)_2(bipy)]$ (pz = pyrazol−1−yl, bipy = 2,2'−bipyridine) shown in Figure 1, undergo spin state switching when stimulated by light, temperature, pressure, or magnetic field. [1-8] The ligand crystal field causes the 3d-orbitals of the central Fe (II) to split into the e_g and t_{2g} orbitals. When the molecule is in the low-spin configuration, the t_{2g} orbital is fully populated by six electrons so that S=0 and diamagnetism are observed. Near and above the critical temperature $T_C \approx 160$ K, the $[Fe(H_2B(pz)_2)_2(bipy)]$ molecule is expected to be in the high-spin state with two unpaired electrons in the e_g orbital and

the remaining four electrons in the t_{2g} orbital, [9] so that S=2. We previously demonstrated that the $[Fe(H_2B(pz)_2)_2(bipy)]$ molecule may undergo a non-volatile, isothermal, reversible spin-state transition even at room temperature when coupled to a ferroelectric thin film.[7, 10] More importantly, the change in conductivity in the SCO molecular layer, which is associated with this spin state transition, provides a facile readout mechanism for potential molecular-based memory devices.[7, 10] This study provides insight into understanding the factors that contribute to spin state retention in the voltage controlled isothermal switching of spin crossover materials, and thus may assist the design of better spintronic devices. When changing the spin state, an energy barrier must be overcome to switch the spin crossover molecule from a low-spin state to a high-spin state or vice versa.[11] Previous work estimated an activation energy of ~60 meV molecule^{-1} (3.55×10^3 kJ m^{-3}) by conducting a time dependent measurement for a $[Fe(H_2B(pz)_2)_2(bipy)]$ thin film on SiO_2.[7, 12] For molecular spin crossover materials and specifically for $[Fe(H_2B(pz)_2)_2(bipy)]$ thin films, multiple studies confirm that the activation energy to change the spin state is significantly reduced by an external magnetic field.[6, 7, 13-20]

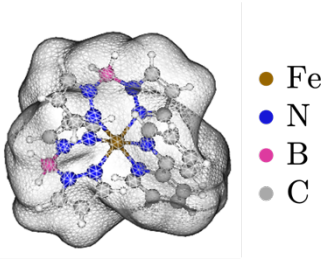

Figure 1. *Octahedral Fe(II) spin crossover molecule $[Fe(H_2B(pz)_2)_2(bipy)]$ (pz = pyrazol−1−yl, bipy = 2,2'−bipyridine) structure with electron distribution.[21] The imperfect symmetry of the six ligands connected to the central Fe (II) ion implies a non-zero orbital moment when the Fe ion is not in the S=0 spin configuration.*

The question arises as to whether the effect of the magnetic field on a spin crossover molecule is influenced by magnetic anisotropy.[22] In other words, does an anisotropic energy barrier exist? Studying the magnetic anisotropy for spin crossover molecules in high-spin states is important for understanding the mechanism of voltage controlled isothermal switching of spin state due to substrate interactions, as well as the observed nonvolatility in the $[Fe(H_2B(pz)_2)_2(bipy)]$ molecular thin films.[7, 8] Furthermore, a better understanding of magnetic anisotropy could provide insights to additional functionality of the molecules within a device context, such as the tuning of the activation energy through substrate interactions.[23, 24] Here, we present a study of the magnetic anisotropy of a spin crossover thin film based on $[Fe(H_2B(pz)_2)_2(bipy)]$ using X-ray magnetic circular dichroism (XMCD). We clearly demonstrate the existence of magnetic anisotropy and determine the spin and orbital contributions to the magnetic anisotropy when the SCO molecules are in the high-spin state.

2. Methods

$[Fe(H_2B(pz)_2)_2(bipy)]$ was synthesized following established methods and its molecular structure with electron distribution envelope is shown in Figure 1.[25, 26] Following previous methods[7, 9], a $[Fe(H_2B(pz)_2)_2(bipy)]$ thin film, measured to be 65 nm thick by a Bruker DektakXT profilometer, was thermally evaporated under high vacuum (3.8×10^{-7} Torr) onto a P/B-doped Si substrate with a native oxide at the surface. The molecule integrity is preserved during this process, as confirmed by the previously published X-ray diffraction data.[27] Field and temperature dependent X-ray magnetic circular dichroism (XMCD) measurements were performed at Argonne National Laboratory's Advanced Photon Source beamline 4-ID-C with a beam diameter of 1 mm in total electron yield mode.[28] Incident X-rays were parallel to the applied magnetic field. Each XMCD spectrum was obtained by first characterizing the sample with left and right circularly polarized light while the magnetic field direction was kept constant, then characterizing the sample again with left and right circularly polarized light and the magnetic field polarity reversed. This technique allows artifacts to be removed from a weak XMCD signal by obtaining a net XMCD signal that is the difference between XMCD spectra obtained with the spin of the photon parallel with either the spin majority or spin minority.

Three XMCD measurements, namely field-orientation dependent XMCD, field-strength dependent XMCD, and temperature-dependent XMCD, were performed to characterize the Fe $L_{2,3}$-edge of the nominally 65 nm thick $[Fe(H_2B(pz)_2)_2(bipy)]$ thin film on a Si substrate with a native SiO_2 oxide surface. These XMCD spectra were then analyzed using the sum rules introduced by Chen *et al*.[29, 30] To obtain the average spin moment $\langle S_z\rangle$ and average orbital moment $\langle L_z\rangle$, we sum the contributions from the $2p_{3/2}$ (L_2) and $2p_{1/2}$ (L_3) orbitals by integrating the XMCD and X-ray absorption spectroscopy (XAS) spectra respectively over the incident photon energy range as shown in Figure 2. We then apply the XMCD sum rule equations $\langle S_z\rangle = -(6p - 4q)(10 - n_{3d})/r$ and $\langle L_z\rangle = -4q(10 - n_{3d})/3r$ where $r = \int(\mu_+ + \mu_-)d\omega$ and $q = \int(\mu_+ - \mu_-)d\omega$ are integrated over the L_3+L_2 edges, and $p = \int(\mu_+ - \mu_-)d\omega$ is integrated over the L_3 edge only.[29, 30] The μ_+ and μ_- values are proportional to the XAS intensities collected with the spin of the photons aligned parallel and anti-parallel to the spin majority respectively. After background subtraction, the XAS signal for each XMCD signal was integrated and the total area under the curve was parameterized as r as shown in Figure 2a. The determination of p and q are shown in Figure 2b, where the error bar for p is the standard deviation of the integrated signal values after the L_3 edge and the error bar for q is the standard deviation

of the integrated signal values after the $L_3 + L_2$ edges. The *p*, *q*, and *r* values are then used in the XMCD sum rules.[29, 30] For Fe (II), the average number of valence electrons in the 3d orbital, n_{3d}, is taken to be 6.61.[29, 31]

3. Results and Discussion

The magnetic moment of the SCO $[Fe(H_2B(pz)_2)_2(bipy)]$ molecule originates from the core Fe (II) ion as indicated in Figure 1. In addition to a spin moment $\langle S_z \rangle$, an Fe (II) SCO molecule in the high-spin state is expected to have a small orbital moment $\langle L_z \rangle$ due to the asymmetry of the ligand field.[11, 32] The details of spin and orbital moment contributions in the $[Fe(H_2B(pz)_2)_2(bipy)]$ molecule are of particular interest. X-ray magnetic circular dichroism is an ideal probe to study the element specific magnetic anisotropy, as it distinguishes between the spin and orbital moment for each molecule.

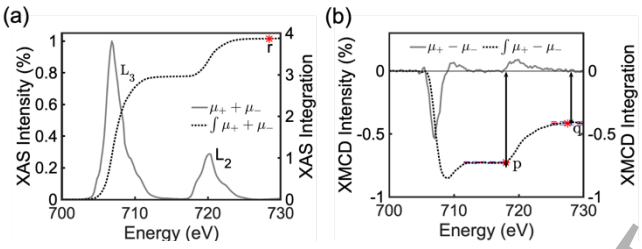

Figure 2. *Analysis of XMCD data. (a) XAS data for the XMCD spectrum obtained with 2.0 T magnetic field normalized by the maximum XAS intensity. The dashed line shows the total integrated area under the solid curve. (b) XMCD spectrum obtained with 2.0 T magnetic field normalized by the maximum XAS intensity. The dashed line shows the total integrated area under the solid line. Determination of p, q, and r values for sum rules are indicated in the figure.*

To obtain the field-orientation dependent XMCD data, a 2.0 T magnetic field was applied approximately parallel to the $[Fe(H_2B(pz)_2)_2(bipy)]$ molecular thin film at temperature of 200 K for the in-plane (IP) measurement and then nearly perpendicular to the sample surface for the out-of-plane (OOP) measurement at the same temperature. Both the in-plane and out-of-plane XMCD spectra are plotted in Figure 3a. The average orbital moment $\langle L_z \rangle$ and spin moment $\langle S_z \rangle$ were calculated for both the in-plane and out-of-plane magnetic field orientations using the XMCD sum rules. These values are plotted as a function of the magnetic field angle in Figure 3b. The orbital moment for the out-of-plane orientation is found to be slightly larger than that of the in-plane orientation, while the spin moment shows a small variation with the opposite trend. The increase in the out-of-plane measurement compared to the in-plane measurement implies that the hard axis for the orbital moment is in-plane. An out-of-plane easy axis suggests that anisotropy is dominated by the magnetocrystalline anisotropy, which in turn suggests certain preferential orientation of $[Fe(H_2B(pz)_2)_2(bipy)]$ in the molecular thin film on the SiO_2 native oxide surface of the Si substrate.[30]

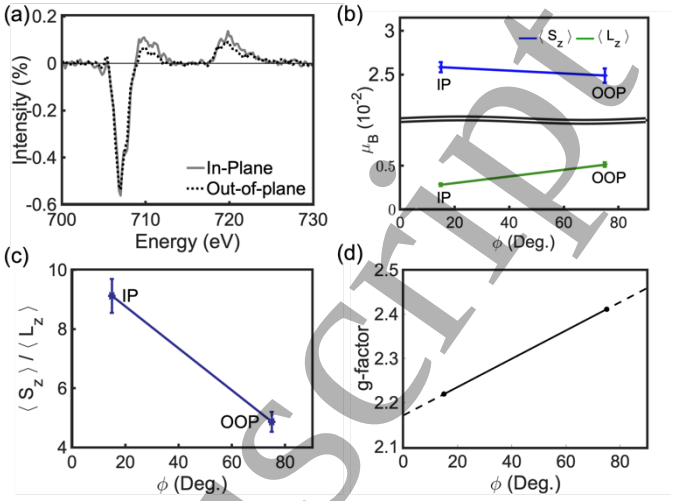

Figure 3. *(a) The XMCD signal for in-plane (IP) and out-of-plane (OOP) field orientation with a field strength of 2 T and temperature of 200 K normalized by the max XAS spectra for each spectrum. (b) The spin moment and orbital moment are plotted separately for both in-plane and out-of-plane applied magnetic field orientations. (c) The ratio of spin to orbital moments for IP and OOP field orientation. (d) Spectroscopic g factor for in-plane and out-of-plane measurements.*

Our data indicate that the orbital moment is locked at some degree relative to the substrate while the spin moment is free to rotate compared to the orbital magnetic moment, implying spin-orbit coupling. Soft X-ray MCD experiments in total electron yield (TEY) mode are surface sensitive with a probing depth of ~2 nm, but substrate effects could still be observed due to cooperative interaction between molecules.[33, 34]

Figure 3c shows the ratio of spin moment to orbital moment for the two different applied magnetic field orientations. The in-plane ratio $\langle S_z \rangle / \langle L_z \rangle$ is almost twice that of the out-of-plane ratio. This is due to the small increase in the orbital moment while the spin moment remains relatively constant, indicating a hard orbital moment and a soft spin moment. Reduced cubic symmetry enhances the orbital moment, and the orbital moment of transition metals is highly sensitive to external fields.[35] Our field-strength dependent XMCD measurement (*vide infra*) shows that the 2.0 T applied magnetic field is far from the saturation field. Therefore, the true orbital moment value of the molecule is expected to potentially be much larger than the average value measured of the thin film sample.[34] Additional measurements for $[Fe(H_2B(pz)_2)_2(bipy)]$ were conducted along the easy axis with the field out-of-plane; the magnitude of the anisotropy values reported from this data are expected to approximate the maximum values possible for the system.

The first order magnetic anisotropy energy density of a thin film is expressed as $E_{ani} = K_1 \sin^2\gamma$, where K_1 is the first

order anisotropy constant and γ is the polar angle as measured from the sample's surface normal.[36] The anisotropy constant K_1 can be further decomposed into the contributions from the shape anisotropy, K_s, and the magnetocrystalline anisotropy, K_u.[36] The shape anisotropy is typically a negative value for thin film samples. The positive anisotropy demonstrated by the magnetic field orientation dependent XMCD data suggests that the anisotropy is dominated by the magnetocrystalline anisotropy rather than the shape anisotropy of the molecule. Using the standard energy expression for spin-orbit coupling, the magnetocrystalline anisotropy energy can be expressed as $\Delta E_{SO} = \zeta [\langle L \cdot S \rangle_{hard} - \langle L \cdot S \rangle_{easy}] = (\zeta/4\mu_B)(m_o^{easy} - m_o^{hard})$ where L is the orbital moment, S is the spin moment, m_o is the orbital moment along the hard or easy axis (in our estimation we used the values shown in Figure 3b), and ζ is the spin-orbit coupling constant with the dimension of energy.[30] Accordingly for our sample, the magnetocrystalline anisotropy has a maximum value when measured along the out-of-plane easy axis.[30] With the spin-orbit coupling constant for Fe (II) ζ = 400 cm^{-1} [37], ΔE_{SO} is estimated to be ~2.47×10^{-5} eV molecule^{-1}. Because the magnetic moment is far from saturation, as the applied magnetic field strength increases the expected energy difference between the hard-axis and soft-axis will remain constant, even as the total energy required to align molecules with the externally applied field increases. Given the average volume of an [Fe(H$_2$B(pz)$_2$)$_2$(bipy)] molecule is 2710 Å^3, the anisotropy constant was determined to be $K_1 = \Delta E_{SO}$ volume-per-molecule^{-1} = 1.47 kJ m^{-3}.[25] This is approximately one-order of magnitude smaller than the previously reported K_1 = 45 kJ m^{-3} value for bulk *bcc*-Fe.[38]

The material dependent spectroscopic *g* factor correlates the spin-orbit coupling and the alignment of the magnetic moment with an external magnetic field. When the molecular z-axis is taken to align with the external magnetic field, the g_z component may be calculated from Kittel's formula expressed as $g_z = 2(\langle L_z \rangle / \langle S_z \rangle + 1)$ where $\langle L_z \rangle$ is the average orbital moment and $\langle S_z \rangle$ is the average spin moment along the z-axis.[39] In Figure 3d, the *g* factor is larger for the out-of-plane measurement than the in-plane measurement. When the external magnetic field is orientated along the out-of-plane direction, the magnetic *g* factor is g_z=2.41. This agrees with the previously reported values for related Fe (II) spin crossover complexes in the high-spin state under a magnetic field.[40, 41]

The spin and orbital moments determined from the XMCD data for [Fe(H$_2$B(pz)$_2$)$_2$(bipy)] thin films are seen to depend on the strength of the externally applied magnetic field. With an out-of-plane magnetic field applied along the easy axis of the orbital moment, the sample was characterized with field magnitudes [0.5 T, 1.0 T, 1.5 T, 2.0 T] at constant temperature T = 200 K with the sample in a high-spin dominated state due to x-ray excitation. The high-spin state fraction is estimated to be near 85% and this is determined by the agreement of the XAS spectra shown in Figure 2a with previously published results. [7] The field-strength dependent XMCD spectra are shown in Figure 4a, where the XMCD signal strength increases with applied field strength for both the L_2 and L_3 edges. In Figure 4b, the spin and orbital moments calculated with the XMCD sum rules show an approximately linear dependence on the applied magnetic field strength. The non-zero y-axis intercept of the $\langle S_z \rangle$ trend line indicates that the magnetic anisotropy favors spontaneous spin moment alignment and therefore the molecule possesses some net spin moment. The non-zero x-axis intercept of the measured orbital moment $\langle L_z \rangle$, as a function of an applied magnetic field, indicates a nonzero critical field. This nonzero critical field for the measured orbital moment implies that an energy barrier is present for orbital moments to align parallel with the external magnetic field in [Fe(H$_2$B(pz)$_2$)$_2$(bipy)] thin films. This indication of an anisotropy barrier has been recently observed in other spin crossover molecular systems.[19]

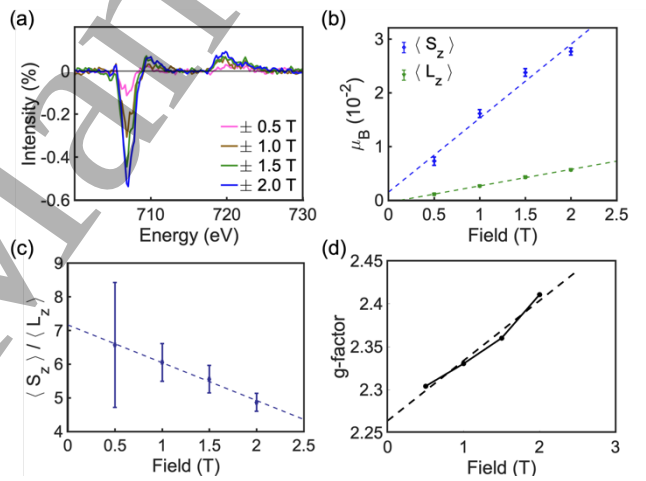

Figure 4*. (a) The XMCD signals for 65 nm [Fe(H$_2$B(pz)$_2$)$_2$(bipy)] on an SiO$_2$ substrate at temperature T = 200 K for various field strengths. (b) The spin and orbital moments as a function of the magnetic field. (c) Ratio of spin moment ⟨S$_z$⟩ to orbital moment ⟨L$_z$⟩ as a function of field strength. (d) The determination of field-dependent g$_z$-factor from the data presented in Figure 4b.*

The anisotropy of the orbital moment in [Fe(H$_2$B(pz)$_2$)$_2$(bipy)] thin films may be determined from the x-axis intercepts of the spin moment and orbital moment trend lines respectively. As shown in Figure 4b, the x-axis intercept indicates the magnitude of the external magnetic field required to overcome the internal energy barrier for a net spin and/or orbital moment of zero. For the spin moment trend line, the x-intercept occurs at -0.11 T, while the orbital moment trend line intercepts the x-axis at +0.13 T. The anisotropy constant can then be determined from $\Delta E = B \cdot \mu$ where ΔE is the energy required to align a magnetic moment

with the external field, μ is the spin or orbital moment of the molecule and B is the magnetic field.[36, 42, 43] The predicted spin moment for an Fe (II) ion is 4.89 μ_B, yielding an energy barrier of 3.11×10^{-2} meV molecule^{-1} with an external field of 0.11 T and a spin-moment anisotropy of 30.9 meV molecule^{-1} (1.83 kJ m^{-3}) when accounting for the volume of a single molecule. This is the same order-of-magnitude as the spin-orbit coupling anisotropy estimated from Figure 3. An orbital moment of 0.668 μ_B is estimated from Kittel's formula for the orbital moment using the predicted spin moment of a single Fe (II) ion s=4.89 μ_B and a g factor of 2.27 (as estimated by the linear trend line in Figure 4d for a field value H = 0.13 T). Applying $\Delta E = B\cdot\mu$ to the predicted orbital moment yields an estimated energy barrier of 5.05×10^{-3} meV molecule^{-1} for a field strength of B = 0.13 T and an orbital-moment anisotropy constant of 5.04 meV molecule^{-1} (0.298 kJ m^{-3}). At zero field, the predicted permanent magnetic moment of the SCO thin film is $\langle m_z\rangle = 8.73\times10^{-27}$ J T^{-1}.

In Figure 4c, the ratio of the spin and orbital moments is shown as a function of an external magnetic field; the size of the error bars decreases as the magnetic field increases due to a better signal-to-noise ratio at a higher field. As field strength increases, the ratio of the spin moment to orbital moment decreases, indicating stronger spin-orbit interaction as the field increases. The g_z factor values determined by Kittel's formula are shown in Figure 4d as a function of field strength with a linear regression, predicting a zero-field g-factor along the z-axis of the thin film to be g_z = 2.26. A typical value for a metal ion with 6 electrons in the d-orbital is g_z = 2.20, while previously reported g factor values for Fe (II) range from 2.2-2.3.[3, 44, 45] The g factor for a Fe (II) ion deviates from the spin-only value of g = 2.00 due to the presence of a small amount of orbital moment. The magnetic anisotropy could be due to various causes including substrate interactions, intermolecular cooperative effects, the inclusion of substrate-induced strain, and a preferential molecular orientation induced by the substrate, but is expected to be temperature dependent regardless of cause.[12, 22, 32] For the temperature-dependent XMCD measurement, the magnetic field strength was kept at 2.0 T and oriented out-of-plane along the orbital moment easy axis. Figure 5a shows the change in the XMCD signal for two temperatures near and slightly above the critical temperature of $[Fe(H_2B(pz)_2)_2(bipy)]$, where the L_3 edge signal decreases with increasing temperature. As thermal energy increases, the SCO molecules experience phonon and magnon effects preventing alignment with the external magnetic field; this causes the net spin moment to decrease due to dynamic spin canting.[46] In Figure 5b, the orbital and spin moments are shown to decrease with increasing temperature, with the spin moment decreasing more quickly than the orbital moment. The $[Fe(H_2B(pz)_2)_2(bipy)]$ thin film is high-spin state dominated for the entire temperature range due to the excitation effects of X-ray source during the measurements.[7, 9, 10] Because the orbital moment of the $[Fe(H_2B(pz)_2)_2(bipy)]$ sample is magnetically hard, the orbital moment demonstrates less temperature dependence.

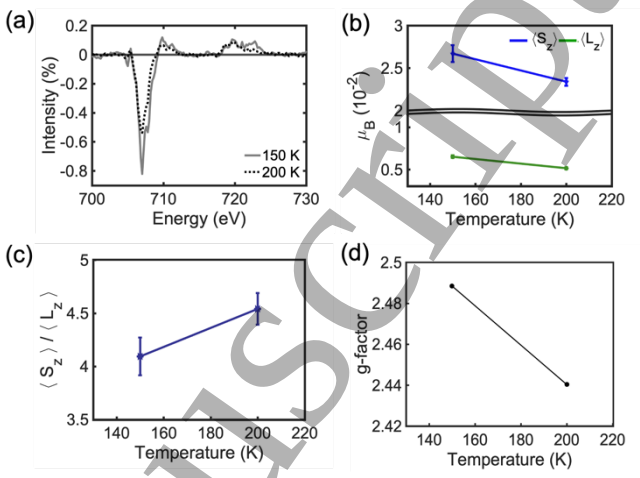

Figure 5. *(a) The XMCD signals for 65 nm $[Fe(H_2B(pz)_2)_2(bipy)]$ on SiO_2 at 2.0 T field strength and temperatures T = 150 K and 200 K. (b) The spin moment (top) and orbital moment (bottom) plotted separately with respect to temperature. (c) The ratio of spin and orbital moments with respect to temperature. (d) The determination of temperature dependent g-factor from data in Figure 5b.*

In Figure 5c, the $\langle S_z\rangle/\langle L_z\rangle$ ratio increases with increasing temperature. The measured orbital moment depends on the orientation of the molecule with respect to the magnetic field and the orientation of the molecule is fixed during deposition due to substrate effects.[34, 47, 48] Here strong interaction between the SCO molecule electric dipole moment and the SiO_2 substrate surface dipole layer is both likely and plausible. This suggests that the orbital moment is insensitive to changes in temperature and confirms that the molecule has a preferential orientation on the substrate as previously reported elsewhere.[48, 49] For a magnetocrystalline anisotropy originating from spin-orbit coupling and substrate effects, there is a possibility of tuning the anisotropy barrier through the use of different substrates.[43]

The magnitude of the K_s and K_u constants for Fe (II) were previously reported to be ~10^{-1} meV atom^{-1} and ~10^{-3} meV atom^{-1} respectively.[30, 38] Our data are in good agreement with these studies. The volume of a single Fe atom is 11.8 Å^3 while the volume of a single $[Fe(H_2B(pz)_2)_2(bipy)]$ molecule is 2710 Å^3 due to the addition of ligands on the central metal ion.[25, 30] The molecule's larger volume results in a decreased coupling between central Fe (II) ions of the $[Fe(H_2B(pz)_2)_2(bipy)]$ molecules. Since the magnetic field from a dipole decreases with a cubic dependency, this provides insight into the origin of the different magnitudes for the magnetic anisotropic constants. Previous studies of $[Fe(H_2B(pz)_2)_2(bipy)]$ in a molecular thin film estimated the activation energy to be ~102 meV molecule^{-1} and

experimentally measured the activation energy to be 60 meV molecule^{-1}.[4, 7, 12] The difference in magnitude between the magnetic anisotropy constants and the activation energy suggests that including crystal field effects and substrate interactions does not substantially change the energy required to change the molecular spin state.

4. Conclusion

Field strength-, field orientation-, and temperature-dependent XMCD studies show that the SCO molecules [$Fe(H_2B(pz)_2)_2(bipy)$] in a thin film have a preferential alignment with the easy axis along the surface normal on the SiO_2 substrate and possess a magnetic anisotropy barrier. The observed magnetic anisotropy dominated by magnetocrystalline anisotropy is due to the coupling between orbital moment and spin moment in the high-spin state, as evidenced by a zero-field g factor of $g_z = 2.26$. The spin-orbit coupling energy is determined to be 1.47 kJ m^{-3} and the spin and orbital moment anisotropies were estimated to be 30.9 and 5.04 meV molecule^{-1}, respectively. The magnetic anisotropy suggests a preferential orientation for the molecule relative to the substrate, but intermolecular interactions and strain could be implicated as well. The spin moment is shown to be soft with respect to external magnetic field orientation and substrate interactions, while the orbital moment shows a preferential direction.

Acknowledgements

This research was supported by the National Science Foundation through NSF-DMR 2003057 [A. S. Dale, S. Yazdani, T. K. Ekanayaka, E. Mishra, R. Cheng, P. A. Dowben]. Use of the Advanced Photon Source was supported by DOE's Office of Science under contract DE-AC02-06CH11357. The synthesis work carried out in the Molecular Foundry, Lawrence Berkeley National Laboratory, was supported by the U.S. Department of Energy (DOE) under contract no. DE-AC02-05CH11231.

References

[1] M. Kondo and K. Yoshizawa, "A theoretical study of spin–orbit coupling in an Fe (II) spin-crossover complex. Mechanism of the LIESST effect," *Chemical physics letters,* vol. 372, no. 3-4, pp. 519-523, 29 April 2003 2003, doi: 10.1016/S0009-2614(03)00431-7.

[2] J.-F. Létard, "Photomagnetism of iron (II) spin crossover complexes—the T (LIESST) approach," *Journal of Materials Chemistry,* vol. 16, no. 26, pp. 2550-2559, 07 March 2006 2006, doi: 10.1039/B603473J.

[3] S. Chorazy *et al.*, "Octacyanidorhenate (V) Ion as an Efficient Linker for Hysteretic Two-Step Iron (II) Spin Crossover Switchable by Temperature, Light, and Pressure," *Angewandte Chemie International Edition,* vol. 59, no. 36, pp. 15741-15749, 02 June 2020 2020, doi: 10.1002/anie.202007327.

[4] A. Galet, A. B. Gaspar, G. Agusti, M. C. Muñoz, G. Levchenko, and J. A. Real, "Pressure effect investigations on the spin crossover systems {Fe [H2B (pz) 2] 2 (bipy)} and {Fe [H2B (pz) 2] 2 (phen)}," *European Journal of Inorganic Chemistry,* Short Communication vol. 2006, no. 18, pp. 3571-3573, September 2006, doi: 10.1002/ejic.200600517.

[5] N. Bouldi *et al.*, "XAS and XMCD Reveal a Cobalt (II) Imide Undergoes High-Pressure-Induced Spin Crossover," *The Journal of Physical Chemistry C,* vol. 126, no. 12, pp. 5784-5792 March 18, 2022 2022, doi: 10.1021/acs.jpcc.2c00614.

[6] G. Hao *et al.*, "Magnetic Field Perturbations to a Soft X-ray-Activated Fe (II) Molecular Spin State Transition," *Magnetochemistry,* vol. 7, no. 10, p. 135, 2021, doi: 10.3390/magnetochemistry7100135.

[7] A. Mosey, A. S. Dale, G. Hao, A. N'Diaye, P. A. Dowben, and R. Cheng, "Quantitative Study of the Energy Changes in Voltage-Controlled Spin Crossover Molecular Thin Films," *The Journal of Physical Chemistry Letters,* vol. 11, no. 19, pp. 8231-8237, 2 September 2020 2020, doi: 10.1021/acs.jpclett.0c02209.

[8] T. K. Ekanayaka *et al.*, "Nonvolatile Voltage Controlled Molecular Spin-State Switching for Memory Applications," *Magnetochemistry,* vol. 7, no. 3, p. 37, 11 March 2021 2021, doi: 10.3390/magnetochemistry7030037.

[9] X. Jiang *et al.*, "Tunable spin-state bistability in a spin crossover molecular complex," *Journal of Physics: Condensed Matter,* vol. 31, no. 31, p. 315401, 22 May 2019 2019, doi: 10.1088/1361-648X/ab1a7d.

[10] G. Hao *et al.*, "Nonvolatile voltage controlled molecular spin state switching," *Applied Physics Letters,* vol. 114, no. 3, p. 032901, 2019, doi: 10.1063/1.5054909.

[11] B. N. Figgis and I. Goodman, *Introduction to ligand fields*. Interscience publishers, 1966.

[12] X. Zhang *et al.*, "Locking and unlocking the molecular spin crossover transition," *Advanced Materials,* vol. 29, no. 39, p. 1702257, 28 August 2017 2017, doi: 10.1002/adma.201702257.

[13] A. Bousseksou *et al.*, "Dynamic triggering of a spin-transition by a pulsed magnetic field," *The European Physical Journal B-Condensed Matter and Complex Systems,* vol. 13, no. 3, pp. 451-456, 2000, doi: 10.1007/s100510050057.

[14] S. Chikara *et al.*, "Magnetoelectric behavior via a spin state transition," *Nature Communications,* vol.

10, no. 1, p. 4043, 2019/09/06 2019, doi: 10.1038/s41467-019-11967-3.

[15] Y. Otsuki, S. Kimura, S. Awaji, and M. Nakano, "Magnetocapacitance effect and magnetostriction by the field-induced spin-crossover in [MnIII (taa)]," *AIP Advances,* vol. 9, no. 8, p. 085219, 2019, doi: 10.1063/1.5097891.

[16] V. B. Jakobsen *et al.*, "Giant magnetoelectric coupling and magnetic-field-induced permanent switching in a spin crossover Mn (III) complex," *Inorganic Chemistry,* vol. 60, no. 9, pp. 6167-6175, 17 December 2020 2020, doi: 10.1021/acs.inorgchem.0c02789.

[17] J.-X. Yu *et al.*, "Three Jahn-Teller States of Matter in Spin-Crossover System Mn (taa)," *Phys Rev Lett,* vol. 124, no. 22, p. 227201, 23 April 2020 2020, doi: 10.1103/PhysRevLett.124.227201.

[18] V. Zapf, P. Sengupta, C. Batista, F. Nasreen, F. Wolff-Fabris, and A. Paduan-Filho, "Magnetoelectric effects in an organometallic quantum magnet," *Physical Review B,* vol. 83, no. 14, p. 140405, 2011, doi: 10.1103/PhysRevB.83.140405.

[19] S. Kimura, Y. Narumi, K. Kindo, M. Nakano, and G.-e. Matsubayashi, "Field-induced spin-crossover transition of [Mn (III) (taa)] studied under pulsed magnetic fields," *Physical Review B,* vol. 72, no. 6, p. 064448, 08/29/ 2005, doi: 10.1103/PhysRevB.72.064448.

[20] X. Zhang *et al.*, "Indications of magnetic coupling effects in spin cross-over molecular thin films," *Chemical Communications,* vol. 54, no. 8, pp. 944-947, 02 January 2018 2018, doi: 10.1039/C7CC08246K.

[21] *MarvinSketch*. (2020). ChemAxon. [Online]. Available: https://chemaxon.com/

[22] T. K. Ekanayaka *et al.*, "Evidence of dynamical effects and critical field in a cobalt spin crossover complex," *Chemical Communications,* 10.1039/D1CC05309D vol. 58, no. 5, pp. 661-664, 2022, doi: 10.1039/D1CC05309D.

[23] C. Gould, K. Pappert, G. Schmidt, and L. W. Molenkamp, "Magnetic Anisotropies and (Ga, Mn) As-based Spintronic Devices," *Advanced Materials,* vol. 19, no. 3, pp. 323-340, 16 January 2007 2007, doi: 10.1002/adma.200600126.

[24] R. Sánchez-de-Armas, N. Montenegro-Pohlhammer, A. Develioglu, E. Burzurí, and C. J. Calzado, "Spin-crossover complexes in nanoscale devices: main ingredients of the molecule–substrate interactions," *Nanoscale,* vol. 13, no. 44, pp. 18702-18713, 2021.

[25] J. A. Real, M. C. Muñoz, J. Faus, and X. Solans, "Spin crossover in novel Dihydrobis (1-pyrazolyl) borate [H2B (pz) 2]-containing Iron (II) complexes. Synthesis, X-ray structure, and magnetic properties of [FeL {H2B (pz) 2} 2](L= 1, 10-Phenanthroline and 2, 2 '-Bipyridine)," *Inorganic chemistry,* vol. 36, no. 14, pp. 3008-3013, 2 July 1997 1997, doi: 10.1021/ic960965c.

[26] X. Zhang *et al.*, "Complexities in the molecular spin crossover transition," *The Journal of Physical Chemistry C,* vol. 119, no. 28, pp. 16293-16302, 24 June 2015 2015, doi: 10.1021/acs.jpcc.5b02220.

[27] S. Yazdani *et al.*, "Optical characterization of isothermal spin state switching in an Fe (II) spin crossover molecular and polymer ferroelectric bilayer," *Journal of Physics: Condensed Matter,* vol. 35, no. 36, p. 365401, 2023, doi: 10.1088/1361-648X/acd7ba.

[28] A. N. Laboratory. "Instrumentation." https://www.aps.anl.gov/Sector-4/4-ID-C/Instrumentation (accessed June 11, 2021).

[29] C. Chen *et al.*, "Experimental confirmation of the X-ray magnetic circular dichroism sum rules for iron and cobalt," *Phys Rev Lett,* vol. 75, no. 1, p. 152, 12 May 1994 1995, doi: 10.1103/PhysRevLett.75.152.

[30] J. Stöhr, "Magnetism : from fundamentals to nanoscale dynamics," H. C. Siegmann, Ed., ed. Berlin ;: Springer, 2006.

[31] L. Honghong, W. Jie, L. Ruipeng, G. Yuxian, W. Feng, and H. Zhiwei, "X-ray magnetic circular dichroism: Orbital and spin moments of iron single-crystal thin film deposited on MgO substrate," *Chinese Science Bulletin,* vol. 50, no. 10, pp. 950-953, 2005, doi: 10.1360/982004-600.

[32] F. J. Arlinghaus and R. A. Reck, "Calculations of the electronic spin and orbital magnetic moments and g′ in ferromagnetic nickel," *Physical Review B,* vol. 11, no. 9, pp. 3488--3490, 1975, doi: 10.1103/PhysRevB.11.3488.

[33] G. Hao *et al.*, "Intermolecular Interaction and Cooperativity in an Fe (II) Spin Crossover Molecular Thin Film System," *Journal of Physics: Condensed Matter,* 2022, doi: 10.1088/1361-648X/ac6cbc.

[34] R. Nakajima, J. Stöhr, and Y. U. Idzerda, "Electron-yield saturation effects in L-edge x-ray magnetic circular dichroism spectra of Fe, Co, and Ni," *Physical Review B,* vol. 59, no. 9, p. 6421, 2 Septemebr 1998 1999, doi: 10.1103/PhysRevB.59.6421.

[35] J. Stöhr and H. König, "Determination of spin-and orbital-moment anisotropies in transition metals by angle-dependent X-ray magnetic circular dichroism," *Phys Rev Lett,* vol. 75, no. 20, p. 3748, 1995.

[36] B. D. Cullity and C. D. Graham, *Introduction to magnetic materials*. John Wiley & Sons, 2011.

[37] G. M. Cole Jr and B. B. Garrett, "Atomic and molecular spin-orbit coupling constants for 3d transition metal ions," *Inorganic Chemistry,* vol. 9, no. 8, pp. 1898-1902, 1970, doi: 10.1021/ic50090a020.

[38] J. Ye *et al.*, "Determination of magnetic anisotropy constants in Fe ultrathin film on vicinal Si (111) by anisotropic magnetoresistance," *Scientific Reports,* vol. 3, no. 1, pp. 1-6, 5 July 2013 2013, doi: 10.1038/srep02148.

[39] A. Meyer and G. Asch, "Experimental g′ and g values of Fe, Co, Ni, and their alloys," *Journal of Applied Physics,* vol. 32, no. 3, pp. S330-S333, 1961, doi: 10.1063/1.2000457.

[40] S. Ossinger, H. Naggert, E. Bill, C. Näther, and F. Tuczek, "Electronic structure, vibrational spectra, and spin-crossover properties of vacuum-evaporable iron (II) bis (dihydrobis (pyrazolyl) borate) complexes with diimine coligands. Origin of giant Raman features," *Inorganic Chemistry,* vol. 58, no. 19, pp. 12873-12887, 17 September 2019 2019, doi: 10.1021/acs.inorgchem.9b01813.

[41] M. Kelai *et al.*, "Robust magnetic anisotropy of a monolayer of hexacoordinate Fe (ii) complexes assembled on Cu (111)," *Inorganic Chemistry Frontiers,* vol. 8, no. 9, pp. 2395-2404, 05 March 2021 2021, doi: 10.1039/D1QI00085C

[42] Z. Hou *et al.*, "Observation of various and spontaneous magnetic skyrmionic bubbles at room temperature in a frustrated kagome magnet with uniaxial magnetic anisotropy," *Advanced Materials,* vol. 29, no. 29, p. 1701144, 2017, doi: 10.1002/adma.201701144.

[43] Q. Xie *et al.*, "Giant enhancements of perpendicular magnetic anisotropy and spin-orbit torque by a MoS2 layer," *Advanced Materials,* vol. 31, no. 21, p. 1900776, 08 April 2019 2019, doi: 10.1002/adma.201900776.

[44] O. Kahn, "Molecular magnetism," *Journal of Chemical Education* vol. 71, no. 1, p. A19, 2021, doi: 10.1021/ed072pA19.2.

[45] T. Smoleński *et al.*, "Magnetic ground state of an individual Fe 2+ ion in strained semiconductor nanostructure," *Nature communications,* vol. 7, no. 1, pp. 1-7, 28 January 2016 2016, doi: 10.1038/ncomms10484.

[46] B. Donnio *et al.*, "Magneto-optical interactions in single-molecule magnets: Low-temperature photon-induced demagnetization," *Solid state sciences,* vol. 12, no. 8, pp. 1307-1313, 2010, doi: 10.1016/j.solidstatesciences.2010.06.003.

[47] M. Gruber *et al.*, "Spin crossover in Fe (phen) 2 (NCS) 2 complexes on metallic surfaces," *The Journal of Chemical Physics,* vol. 146, no. 9, p. 092312, 2017, doi: 10.1063/1.4973511.

[48] S. Beniwal *et al.*, "Surface-induced spin state locking of the [Fe (H2B (pz) 2) 2 (bipy)] spin crossover complex," *Journal of Physics: Condensed Matter,* vol. 28, no. 20, p. 206002, 2016, doi: 10.1088/0953-8984/28/20/206002.

[49] S. Ossinger *et al.*, "Vacuum-evaporable spin-crossover complexes in direct contact with a solid surface: Bismuth versus gold," *The Journal of Physical Chemistry C,* vol. 121, no. 2, pp. 1210-1219, 21 December 2016 2017, doi: 10.1021/acs.jpcc.6b10888.